

# Weathering rates as a function of flow through an alpine soil

D.W. Clow<sup>a,\*</sup>, J.I. Drever<sup>b</sup>

<sup>a</sup> U.S. Geological Survey, MS 415, Box 25046, Denver Federal Center, Lakewood, CO 80225-0046, USA

<sup>b</sup> Department of Geology and Geophysics, University of Wyoming, Laramie, WY 82071-3006, USA

Received 6 June 1995; accepted 2 November 1995

---

## Abstract

The effect of flow on release rates of solutes from soil in a 39-m<sup>2</sup> alpine catchment in the Colorado Rockies was measured during the summers of 1990–1994. Flow rates through the soil were varied by augmenting natural rainfall with deionized irrigation water. Daily water inputs averaged between 96 and 216 l day<sup>-1</sup> during the five field seasons, and mean discharge (inputs minus evapotranspiration) varied from 35 to 175 l day<sup>-1</sup>. Volume-weighted mean concentrations of base cations and silica decreased only moderately in response to the increased water inputs. Input fluxes of solutes in precipitation were similar in each of the study seasons, but output fluxes of base cations and silica in surface outflow increased substantially in conjunction with the average water input rate for the season.

Weathering rates calculated from the chemical fluxes increased substantially in response to increases in water input rates. The increases appear to be largely attributable to enhanced transport of solutes from the soil matrix under high flow conditions. At high flow, physical flushing of micropores presumably occurs to a greater extent than during low-flow periods because of greater soil wetness and higher hydrologic head. Increased flushing would also cause an increased rate of diffusion of solutes from microcracks in mineral surfaces and constricted pore spaces in response to an increased concentration gradient between those regions and adjacent areas in the soil matrix. Another consequence of the increased flushing that occurs during periods of high flow is that concentrations throughout the soil matrix tend to be lower, which might increase chemical weathering rates of some silicate minerals such as microcline, which are relatively close to saturation. Decreased Si concentrations under high-flow conditions appear to promote dissolution of amorphous aluminosilicates or desorption of Si from mineral surfaces, buffering Si concentrations in the soil solutions. Thus, both physical transport of solutes and subsequent chemical effects appear to be responsible for the positive relation observed between fluxes of weathering products and water input rates.

---

## 1. Introduction

Silicate weathering plays an important role in mitigating the effects of a variety of anthropogenic activities on terrestrial ecosystems. Weathering reactions consume some of the potentially harmful products of fossil fuel combustion and other industrial

pursuits, such as CO<sub>2</sub> and strong acids in polluted rain and snow. In the long-term, the ability of natural systems to regulate CO<sub>2</sub> in the atmosphere or neutralize acid deposition is limited by the kinetics of silicate weathering reactions. Models that seek to accurately predict long-term trends in atmospheric CO<sub>2</sub> or the response of ecosystems to various levels of acid deposition should include silicate weathering rates as inputs. Environmental variables such as pre-

---

\* Corresponding author.

precipitation amount and temperature might exert considerable control on weathering rates and chemical fluxes of weathering products from watersheds (White and Blum, 1995), but the magnitude of those effects have not been well quantified.

The purpose of this paper is to present results from a field study in which chemical weathering rates were measured under varying hydrologic conditions at a small high-elevation catchment in the Rocky Mountains, U.S.A. Weathering rates were calculated using the mass-balance technique (Garrels and Mackenzie, 1967) for five summer seasons (July through September, 1990–1994). Flow rates through the soil were varied by augmenting natural rainfall with deionized irrigation water.

The study site is located in Loch Vale, a glaciated alpine–subalpine drainage basin in Rocky Mountain National Park, about 80 km northwest of Denver, Colorado. The 39-m<sup>2</sup> study catchment, referred to locally as the “nanocatchment”, is situated on a small bedrock knoll above treeline at 3300-m elevation above sea-level. It consists of gently sloping bedrock with a 15.5-m<sup>2</sup> pocket of soil at its center. Outflow leaves the nanocatchment via a narrow crack in the bedrock at the northern boundary. Soil depth was probed on a 0.25-m grid; the average soil depth was 0.3 m, the maximum depth was 0.7 m, and the soil volume was 3.35 m<sup>3</sup>. Vegetation is characteristic of alpine tundra in the Rockies, consisting of sparse short herbs and grasses. By using a small, hydrologically tight catchment with minimal vegetation, it was possible to minimize errors in solute flux and weathering rate calculations associated with the water balance, mineral surface-area measurements, and biological uptake and release of nutrients.

Bedrock consists of granite and granitic gneiss, which are composed primarily of quartz, oligoclase (An<sub>27</sub>), biotite, and microcline (Cole, 1977; Brad-dock and Cole, 1990). Post-metamorphic alteration resulted in some conversion of biotite to chlorite (Cole, 1977), and microscopic hydrothermal calcite has been identified in the Loch Vale watershed by Mast et al. (1990). Soil at the nanocatchment is a Cryochrept, an immature, cold soil developed from glacial till deposited during the Pinedale glaciation between 7,600 and 12,000 years ago (Madole, 1976; Birkeland et al., 1987). Primary minerals in the soil are identical to the local bedrock (Baron et al., 1992;

this study); the < 2-μm fraction consists chiefly of smectite, mixed-layer smectite–illite, kaolinite, biotite, and chlorite (Mast et al., 1990).

Climate at the nanocatchment is typical of high-elevation tundra in the Rocky Mountains of Colorado. Summers are cool, with frequent afternoon thunderstorms; winters are cold and windy, allowing the ground to freeze between October and May. Soil temperatures at the nanocatchment generally ranged from 7° to 11°C during the period of study.

## 2. Methods

### 2.1. Mass-balance calculations

Weathering rates at the field site were calculated for the July through September periods of 1990–1994 using the mass-balance technique described by Garrels and Mackenzie (1967). Mass-balance calculations use an accounting system to estimate the amount of solutes that are derived from specific sources. A simple solute mass-balance equation has the form:

$$\begin{aligned} &(\text{atmospheric inputs}) + (\text{weathering}) \\ &= (\text{outflow}) \pm (\text{changes in soil storage}) \\ &\pm (\text{biological uptake and/or release}) \end{aligned}$$

It is possible to solve for the weathering term if atmospheric inputs, outflow fluxes, and changes in storage are known, and if the balance between biological uptake and release is in a steady state. Wet deposition inputs were calculated from weekly wet-fall chemistry measurements made by the National Atmospheric Deposition Program/National Trends Network (Network, 1984–1994, NADP/NTN) at a site 0.8 km north and 180 m below the nanocatchment and from rainfall volumes measured in two rain gages located at the nanocatchment boundaries. Dry deposition of base cations and Si were not included in the input fluxes because those solutes are primarily deposited as dust particles (Gatz et al., 1986), and thus are part of the mineral weathering system. Soil at the study site was irrigated at a fixed rate (except during equipment breakdowns) with deionized water, which was manufactured on-site by passing stream water through ion-exchange columns with activated carbon to remove Si. Irrigation promoted a more

continuous flow through the soil than would occur under natural conditions and provided the ability to vary the rate of water inputs without altering chemical inputs. The volume of deionized water added was measured using a recording tipping bucket and data-logger system.

Fluxes of solutes leaving the nanocatchment were calculated by multiplying the weekly outflow volume times the solute concentrations measured in weekly outflow water samples. Weekly outflow volumes were calculated by subtracting evapotranspiration (ET) losses from the weekly inflow volume. Analytical techniques and quality assurance methods for water samples are presented in detail by Clow (1992). Daily samples collected for a one-month period (August 1994) displayed little short-term variability in composition, indicating that the weekly sampling frequency was sufficient to characterize the outflow chemistry for the purpose of making flux calculations. Evapotranspiration was calculated using a modified form of the Penman equation (Penman, 1948), taking into account differences between potential and actual ET (Clow, 1992). The Penman equation uses a simple energy balance combined with a mass-transfer term that accounts for wind speed and humidity. Radiation, wind speed, and humidity were measured at a weather station located adjacent to the NADP/NTN site in Loch Vale. Estimates of outflow volumes calculated using the Penman equation agreed to within  $\pm 3\%$  of direct measurements made in 1991 using a recording tipping bucket.

The storage term in the mass-balance equation includes solutes that are in soil solutions, on exchange sites, and present in biomass. As a first approximation, biomass and cation exchange pools were assumed to be at steady state. This assumption probably is most reasonable for  $\text{Na}^+$  and Si because neither are a major component of either the biomass or cation exchange pools in tundra ecosystems (Lovering and Engel, 1967; Arthur, 1992). The lack of extensive vegetation at the nanocatchment supports the assumption that biologic effects were minimal. Weathering rates for plagioclase were based on  $\text{Na}^+$  and Si fluxes (see below), so rates calculated for this mineral were least dependent on the assumption of minimal biologic or exchange effects. Changes in the mass of solutes stored in soil solution were

calculated based on beginning and end of the season concentrations in samples collected from suction soil lysimeters. The volume of water stored in the soil was approximately equal at the beginning and end of each field season based on depth-to-water measurements made weekly in six piezometers located at the nanocatchment.

The dominant weathering reactions in the Loch Vale watershed have been well defined by Mast et al. (1990), who measured primary mineral compositions, identified weathering products, and calculated a mass balance for the entire Loch Vale watershed. The weathering reactions written by Mast et al. (1990) were used in this study for the mass-balance calculations, except that microcline was added to the list of possible reactants because laboratory experiments involving dissolution of minerals obtained from nanocatchment-area soils indicated that fluxes from microcline weathering might be significant (Clow, 1992).

Only a brief outline of the mass-balance procedure is provided here; for more details see Garrels and Mackenzie (1967), Mast et al. (1990), and Clow (1992). After calculating net solute fluxes from the nanocatchment by subtracting precipitation inputs from outflow fluxes and accounting for changes in storage in soil solutions, solutes were assigned to specific weathering reactions.  $\text{Mg}^{2+}$  and  $\text{K}^+$  were attributed to weathering of biotite and chlorite to a mixed-layer smectite clay containing  $\sim 30\%$  illite layers (Mast et al., 1990). It was assumed that this weathering reaction released  $\text{Mg}^{2+}$  and  $\text{K}^+$  in a 2:1 ratio because that was the ratio observed in laboratory dissolution experiments conducted on a biotite/chlorite concentrate obtained from soil adjacent to the nanocatchment (Clow, 1992). Any remaining  $\text{K}^+$  was assigned to weathering of microcline to kaolinite. Next,  $\text{Na}^+$  was assigned to weathering of oligoclase ( $\text{An}_{27}$ ) to kaolinite. Kaolinite was used as the secondary phase for simplicity; much of the material assigned to formation of kaolinite probably actually forms a metastable amorphous aluminosilicate with a composition similar to kaolinite (see discussion below). Some of the amorphous material presumably converts to crystalline kaolinite over time, but some of it apparently redissolves, forming gibbsite and releasing Si to solution. This is indicated by an excess of Si in solution beyond the

amount that can be ascribed to weathering of feldspars to kaolinite; the weathering rate of quartz under Earth-surface conditions has been found to be quite small relative to feldspars and mica (Brady and Walther, 1990), so its contribution to the net solute flux was assumed negligible. There also was considerably more  $\text{Ca}^{2+}$  than could be accounted for by weathering of oligoclase — for simplicity the excess  $\text{Ca}^{2+}$  was assigned to calcite weathering; release of  $\text{Ca}^{2+}$  from the cation exchange pool is also plausible.

## 2.2. Mineral percentages

Integrated soil samples were collected from the A, upper B, and lower B soil horizons in a soil pit dug adjacent to the nanocatchment. Bulk density and grain-size distributions were measured on each of the three soil samples according to methods outlined in Jackson (1969) [see Clow (1992) for more details]. The mass of soil in each of the soil horizons at the nanocatchment was estimated from the soil-volume measurements made by probing and bulk densities measured on the soil samples. Mineral percentages were determined for four particle-size fractions (2–53-, 53–106-, 106–208-, and 208–2000- $\mu\text{m}$  diameter) of each soil horizon by point counting using a combination of optical microscopy with stained thin-sections and scanning electron microscopy with energy-dispersive X-ray spectrometry. Mineral percentages in the < 2- $\mu\text{m}$  size-fraction were estimated from bulk chemical analyses and X-ray diffraction data presented in Mast (1989) using the technique described by Swoboda-Colberg and Drever (1993). Biotite and chlorite grains were intergrown due to hydrothermal replacement of biotite by chlorite, making it impossible to quantify their mineral percentages separately; for this reason, the two minerals were lumped. The small grain size of calcite and kaolinite precluded assigning mineral percentages to those minerals. Combining soil mass data with the mineral percentage data yielded a matrix describing the mass of quartz, oligoclase, microcline, and biotite/chlorite in five size-fractions of three soil horizons. The results for the three soil horizons were summed to obtain the total masses of each mineral in the nanocatchment soil (Table 1).

## 2.3. Surface area calculations

To facilitate surface-area measurements, the particle-size fractions were processed to remove organic matter (30% hydrogen peroxide) and iron oxide coatings (sodium citrate/sodium dithionite) (Jackson, 1969). A subsample of the 106–208- $\mu\text{m}$  size-fraction was then separated into a biotite/chlorite concentrate and a feldspar/quartz concentrate using heavy liquids and a magnetic separator. The specific surface areas ( $\text{m}^2 \text{g}^{-1}$ ) of the mineral concentrates and the particle-size fractions were measured using the three-point  $\text{N}_2$  BET method (Brunauer et al., 1938) to obtain a mathematical relation between specific surface area, mineral type, and grain size (Table 1). The relation was used to estimate specific surface areas for feldspars and biotite/chlorite in particle-size fractions other than the 106–208- $\mu\text{m}$  fraction, and is expressed as:

$$(\text{SSA}_{\text{bulk},x} / \text{SSA}_{\text{bulk},106-208}) \times \text{SSA}_{y,106-208}$$

Table 1

Mass, specific surface area, and total surface area of selected minerals in nanocatchment soil

	Particle size fraction (μm)					Total
	0–2	2–53	53–106	106–208	208–2000	
<i>Mineral mass (kg):</i>						
Quartz	40	109	162	142	471	923
Oligoclase	13	93	166	92	389	752
Microcline	13	54	131	133	382	713
Biotite/ chlorite	27	121	100	99	348	694
Other	174	35	55	38	251	552
Total	267	412	612	502	1841	3635
<i>Specific surface area (m<sup>2</sup> g<sup>-1</sup>):</i>						
Oligoclase	0.61	0.35	0.27	0.21 <sup>a</sup>	0.05	
Microcline	0.61	0.35	0.27	0.21 <sup>a</sup>	0.05	
Biotite/chlorite	9.27	5.37	4.04	3.20 <sup>a</sup>	0.78	
Bulk	2.32 <sup>a</sup>	1.34 <sup>a</sup>	1.01 <sup>a</sup>	0.80 <sup>a</sup>	0.20 <sup>a</sup>	
<i>Total surface area (m<sup>2</sup>):</i>						
Oligoclase	8	33	44	19	20	124
Microcline	8	19	35	28	20	109
Biotite/ chlorite	248	652	402	316	273	1891

<sup>a</sup> indicates specific surface area was measured. All other specific surface areas were calculated (see text).

where SSA is the specific surface area; “bulk” refers to particle-size fractions not subdivided into mineral concentrates;  $x$  is a given particle-size fraction;  $y$  is a given mineral; and 106–208 refers to the 106–208- $\mu\text{m}$  particle-size fraction. For example, the specific surface area of biotite/chlorite in the 53–106- $\mu\text{m}$  fraction =  $(1.01/0.80) \times 3.20 = 4.04$ . The masses of oligoclase, microcline, and biotite/chlorite in each size-fraction were multiplied times the appropriate specific surface area to obtain the total surface areas of those minerals in the nanocatchment soil (Table 1). It was assumed that quartz, oligoclase, and microcline all had the same specific surface areas.

### 3. Results and discussion

Mean daily precipitation ranged from 63 to 102  $\text{l day}^{-1}$  (1.6 to 2.6  $\text{mm day}^{-1}$ ), and irrigation with deionized water contributed an average of 18 to 114  $\text{l day}^{-1}$  (0.5 to 2.9  $\text{mm day}^{-1}$ ) during the five field seasons (Table 2). Evapotranspiration losses ranged from 38 to 60  $\text{l day}^{-1}$  (1.0 to 1.5  $\text{mm day}^{-1}$ ). Mean seasonal discharge, which is the average of the daily discharges for a given field season (July–September in this study), ranged from 35 to 175  $\text{l day}^{-1}$  (0.9 to 4.5  $\text{mm day}^{-1}$ ), and roughly correlated with water inputs (Fig. 1a). Soils were continuously wet throughout all field seasons and were saturated to within 0 to 10 cm below the soil surface depending on water input rates; the saturation level tended to be higher when water input rates were high.

Precipitation was mildly acidic, with volume-weighted mean (VWM)  $\text{H}^+$  concentrations ranging

Table 2  
Mean daily water fluxes at nanocatchment

	Rainfall ( $\text{l day}^{-1}$ )	Irrigation ( $\text{l day}^{-1}$ )	Evapotran- spiration ( $\text{l day}^{-1}$ )	Discharge ( $\text{l day}^{-1}$ )	Discharge ( $\text{mm day}^{-1}$ )
1990	78	18	60	35	0.90
1991	102	111	59	154	3.95
1992	88	89	38	139	3.56
1993	102	114	41	175	4.49
1994	63	83	47	99	2.54

To obtain water fluxes in units of  $\text{mm day}^{-1}$ , divide fluxes in  $\text{l day}^{-1}$  by the nanocatchment area in square meters (39).

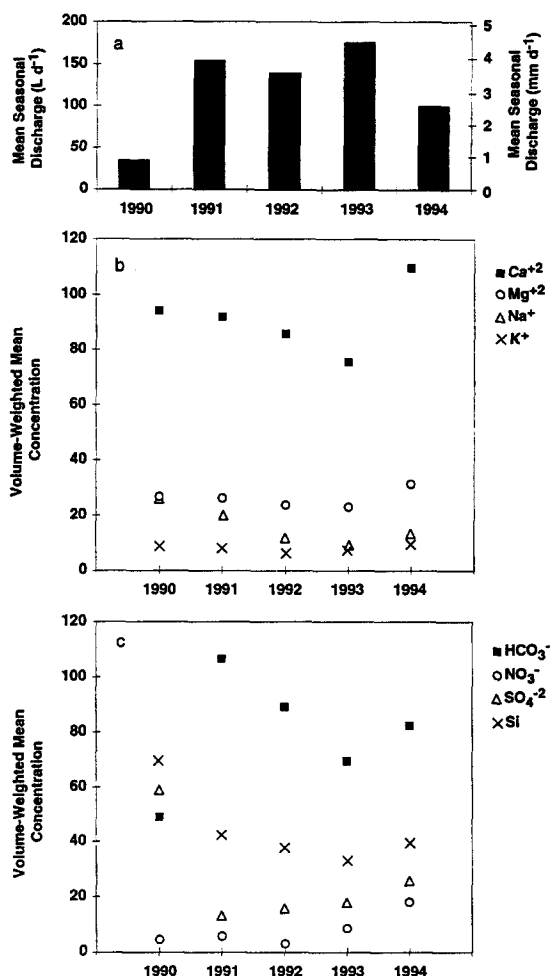


Fig. 1. a. Mean daily discharge for each year of study. b. Volume-weighted mean concentrations of cations in nanocatchment outflow. c. Volume-weighted mean concentrations of anions and Si in nanocatchment outflow. Units are  $\mu\text{eq l}^{-1}$  for cations and anions, and  $\mu\text{mol l}^{-1}$  for Si.

from 10.1 to 15.4  $\mu\text{eq l}^{-1}$  (pH 4.8 to 5.0) (Table 3).  $\text{NH}_4^+$  was the other major cation, and the dominant anions were  $\text{NO}_3^-$  and  $\text{SO}_4^{2-}$ . Solute concentrations in irrigation water were  $< 2 \mu\text{eq l}^{-1}$  for all charged constituents, and  $< 5 \mu\text{mol l}^{-1}$  for Si.  $\text{Ca}^{2+}$  was the major cation in outflow solutions, followed by  $\text{Mg}^{2+}$ ,  $\text{Na}^+$ , and  $\text{K}^+$  (Table 3; Fig. 1b).  $\text{HCO}_3^-$  was generally the dominant anion, followed by  $\text{SO}_4^{2-}$  and  $\text{NO}_3^-$  (Fig. 1c). A consistent excess of cations in the charge balance of 5–15% indicates that organic an-

ions were a small component of the outflow solutions.

VWM concentrations of weathering products (base cations,  $\text{HCO}_3^-$ , and Si) were considerably higher in outflow solutions than in precipitation or irrigation water, presumably due to interactions between input water and geologic materials (Table 3) (Si concentrations are not measured in precipitation by the NADP/NTN, but have been measured in other Loch Vale studies, and have consistently been below the detection limit of  $5 \mu\text{mol l}^{-1}$ ; Clow and Mast, 1995). After an initial pulse of  $\text{NO}_3^-$  in the first outflow water of each season, concentrations of  $\text{NH}_4^+$  and  $\text{NO}_3^-$  generally were lower in outflow solutions than in precipitation, indicating consumption of these nutrients by biologic activity in the soil. The initial pulse of  $\text{NO}_3^-$  generally was accompanied by a pulse of  $\text{Ca}^{2+}$ , and to a lesser extent other cations, and probably was attributable to flushing of biologic decay products that accumulated in the nanocatchment soil over the winter. Concentrations of  $\text{SO}_4^{2-}$  in outflow solutions were much higher than in precipitation during years when water input rates were low, but were similar to precipitation in relatively wet years. Concentrations of  $\text{Cl}^-$  in outflow solutions generally were about double the concentrations measured in precipitation, which for most years was considerably higher than could be attributed to evap-

otranspiration based on the water budget. Dry deposition or weathering of  $\text{Cl}^-$  from an unidentified mineral source are plausible sources of the excess  $\text{Cl}^-$ .

VWM concentrations of base cations and Si decreased only slightly in response to increasing mean seasonal discharge (Fig. 2), indicating that geochemical processes in the soil tended to mitigate the dilution effect attributable to irrigation and precipitation inputs. VWM concentrations of  $\text{NO}_3^-$  were invariant with discharge; this might be due to  $\text{NO}_3^-$  being a limiting nutrient for tundra vegetation at the nanocatchment. VWM concentrations of  $\text{SO}_4^{2-}$  exhibited a strong inverse relation to mean seasonal discharge, perhaps reflecting dilution of atmospheric inputs of strong acids in wet years.  $\text{HCO}_3^-$  increased with increasing mean seasonal discharge (Fig. 2b), reflecting the fact that strong acid concentrations decreased substantially while base cation concentrations decreased only slightly.

Fluxes of weathering products in outflow water exhibited a strong positive relation to mean seasonal discharge (Table 4, Fig. 3). Since fluxes are equal to concentration times discharge, this is consistent with the relatively small decreases in VWM concentrations of weathering products coupled with large increases in the amount of water leaving the system.

Weathering rates, as calculated from net solute

Table 3

Volume-weighted mean concentrations of precipitation (National Atmospheric Deposition Program/National Trends Network, 1990–1994) and outflow water at nanocatchment (units are  $\mu\text{eq l}^{-1}$ , except Si, which is in  $\mu\text{mol l}^{-1}$ ; n.a. = not analyzed)

Year	$\text{H}^+$	$\text{Ca}^{2+}$	$\text{Mg}^{2+}$	$\text{Na}^+$	$\text{K}^+$	$\text{NH}_4^+$	$\text{NO}_3^-$	$\text{SO}_4^{2-}$	$\text{Cl}^-$	$\text{HCO}_3^-$	Si
<i>Precipitation chemistry:</i>											
1990	10.1	6.1	1.4	1.3	0.5	13.3	15.2	15.4	2.7		
1991	15.4	4.6	0.9	1.0	0.3	8.0	13.9	14.2	1.6		
1992	14.9	7.2	1.6	2.4	0.7	10.6	14.4	16.3	2.5		
1993	11.1	6.5	1.6	2.8	0.7	8.6	11.8	13.1	2.4		
1994	15.3	8.0	1.9	1.8	0.9	12.6	17.5	16.5	2.4		
<i>Outflow chemistry:</i>											
1990	0.1	94.2	26.2	25.8	9.4	n.a.	4.5	58.8	6.9	49.0	70.8
1991	0.1	91.9	27.0	19.3	8.5	n.a.	5.8	13.1	5.4	106.4	43.7
1992	0.1	85.7	22.6	11.2	6.4	1.4	3.0	15.6	5.3	88.9	39.1
1993	0.1	75.3	21.0	8.7	8.0	1.6	8.6	17.9	5.5	69.3	34.3
1994	0.2	109.8	32.9	13.4	10.0	2.4	18.1	25.7	5.3	82.3	40.8

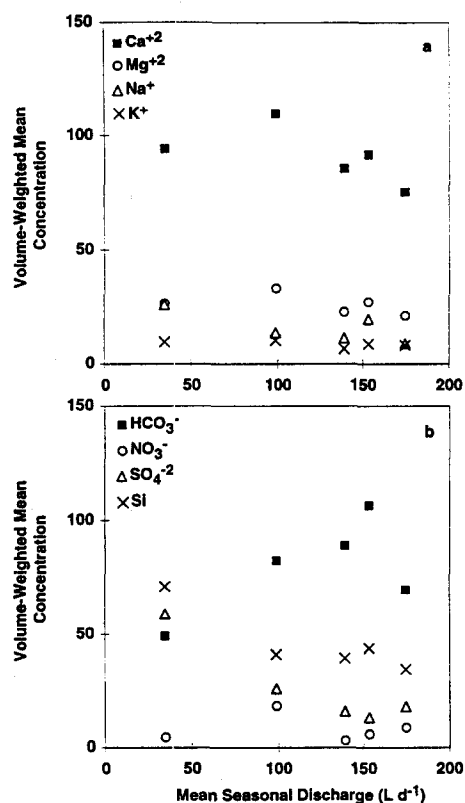


Fig. 2. a. Volume-weighted mean concentrations of cations in nanocatchment outflow as a function of mean seasonal discharge. b. Volume-weighted mean concentrations of anions and Si in nanocatchment outflow as a function of mean seasonal discharge. Units are  $\mu\text{eq l}^{-1}$  for cations and anions, and  $\mu\text{mol l}^{-1}$  for Si.

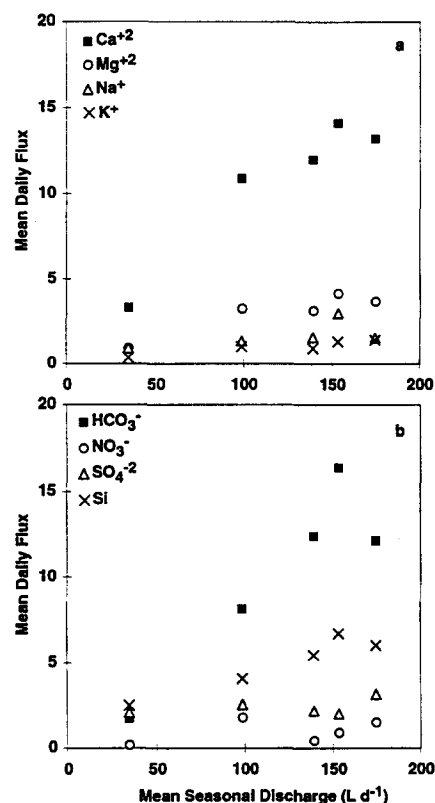


Fig. 3. a. Mean daily flux of cations in outflow as a function of mean seasonal discharge. b. Mean daily flux of anions and Si in outflow as a function of mean seasonal discharge. Units are  $\text{meq day}^{-1}$  for cations and anions, and  $\text{mmol day}^{-1}$  for Si.

Table 4

Mean daily fluxes in precipitation (National Atmospheric Deposition Program/National Trends Network, 1990–1994) and outflow water at nanocatchment (units are  $\text{meq day}^{-1}$ , except Si, which is in  $\text{mmol day}^{-1}$ ; n.a. = not analyzed)

	$\text{H}^+$	$\text{Ca}^{2+}$	$\text{Mg}^{2+}$	$\text{Na}^+$	$\text{K}^+$	$\text{NH}_4^+$	$\text{NO}_3^-$	$\text{SO}_4^{2-}$	$\text{Cl}^-$	$\text{HCO}_3^-$	Si
<i>Precipitation fluxes:</i>											
1990	1.0	0.6	0.1	0.1	0.1	1.4	1.6	1.6	0.3		
1991	1.8	0.5	0.1	0.1	0.0	0.9	1.6	1.7	0.2		
1992	1.5	0.7	0.2	0.3	0.1	1.1	1.5	1.7	0.3		
1993	0.8	0.5	0.1	0.2	0.1	0.6	0.9	1.0	0.2		
1994	1.7	0.9	0.2	0.2	0.1	1.4	1.9	1.8	0.3		
<i>Outflow fluxes:</i>											
1990	< 0.1	3.2	0.9	0.9	0.3	n.a.	0.2	2.0	0.2	1.7	2.4
1991	< 0.1	14.1	4.1	3.0	1.3	n.a.	0.9	2.0	0.8	16.3	6.7
1992	< 0.1	11.9	3.1	1.6	0.9	0.2	0.4	2.2	0.7	12.4	5.4
1993	< 0.1	13.2	3.7	1.5	1.4	0.3	1.5	3.1	1.0	12.1	6.0
1994	< 0.1	10.9	3.3	1.3	1.0	0.2	1.8	2.5	0.5	8.1	4.0

fluxes, were positively related to mean seasonal discharge (Table 5, Fig. 4). Calcite and biotite weathering rates exhibited the greatest response to changes in mean seasonal discharge (Fig. 4). Weathering rates calculated for the entire Loch Vale watershed by Mast (1992) were within the range of those measured at the nanocatchment (Table 5), providing some indication of the validity of the calculated weathering rates at the nanocatchment.

Weathering rates at the nanocatchment, expressed per unit mineral surface area (Table 6), were similar to those measured in column experiments in the laboratory at 19°C using the cleaned 106–208- $\mu\text{m}$  particle-size fraction of soil collected near the nanocatchment. Dissolution rates measured on the same material using fluidized-bed reactors were substantially higher (Table 6). The higher rates obtained in the fluidized-bed reactors were attributed to differences in the hydrologic environment in the two experimental systems; other variables such as temperature, type of reactant solutions, and saturation state were essentially the same. In the columns the mineral grains were at rest, but in the fluidized-bed reactors the grains were kept in suspension by a jet of fluid at the bottom of the reactor. It was hypothesized that all mineral surfaces were in contact with moving water in the fluidized bed reactors, whereas flowing water in the columns did not contact all surfaces. It was also noted that the hydrologic environment in the column apparatus might be more representative of nature.

The positive relation between mean seasonal dis-

charge and fluxes of weathering products at the nanocatchment could be due to a variety of physical and chemical processes. Physical processes that might be partly responsible for increased fluxes of weathering products during wet years included increased flushing and diffusion. Flushing of solutes from soil micropores could be accentuated under high flow conditions. Recent work has established the existence of a two-domain system in many soil environments (Beven and Germann, 1982; Hornberger et al., 1990; Brusseau, 1993); rapid flow occurs through macropores, and soil solutions move much more slowly through the soil matrix (micropores). Solute concentrations are likely to be relatively high in the micropores because of the longer residence time. During years of high water inputs (wet years) and concomitant high flow rates through the soil, flushing of solutes from micropores should increase. In the unsaturated zone, this is because water movement increases as soil wetness increases (Hornberger et al., 1990), and in the saturated zone, it is because flow is promoted by increased hydrologic head (Linsley et al., 1982). Thus, during periods of high flow rates increased flushing of relatively concentrated micropore water could help maintain solute concentrations in the nanocatchment outflow water. This idea of variable flushing efficiency is similar to the hypothesis of Velbel (1993) and Swoboda-Colberg and Drever (1993), who postulated that because of heterogeneous flow through soils, only a fraction of the total mineral surface area generally is in contact with moving water, and thus the effective mineral

Table 5

Weathering rates of minerals ( $\text{mol ha}^{-1} \text{ yr}^{-1}$ ) in nanocatchment soil expressed relative to land area (n.i. = mineral not included in mass-balance calculations)

	Discharge ( $\text{mm day}^{-1}$ )	Oligoclase	Biotite	K-spar	Chlorite	Kaolinite <sup>a</sup>	Calcite
Nanocatchment							
1990	0.90	83	30	5	15	41	96
1991	3.95	299	162	17	81	98	518
1992	3.56	127	118	3	59	167	460
1993	4.49	148	150	40	75	152	530
1994	2.54	111	126	10	63	113	416
Loch Vale <sup>b</sup>	2.25	99	29	ni	7	18	106

<sup>a</sup> Refers to crystalline kaolinite plus amorphous aluminosilicates with the composition of kaolinite.

<sup>b</sup> Source: Discharge data from J. Baron (pers. commun., 1995). Weathering rates from Mast (1992). Data for Loch Vale represent four-year average for 1984, 1986, 1987, and 1988.



surface area often is much lower than the total mineral surface area.

Diffusion of solutes from poorly connected micropores, 'dead end' pore spaces, and microcracks in mineral surfaces is another physical process that could be enhanced when flow rates are high. Over a hydrologic season, concentrations in the soil matrix decline as solutes are flushed; this is indicated by a decrease in soil solution concentrations observed

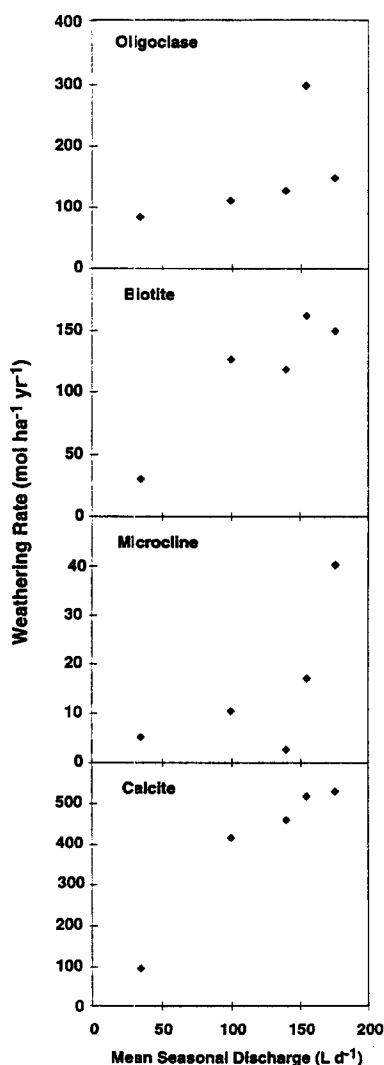


Fig. 4. Weathering rates of oligoclase, biotite, microcline, and calcite at the nanocatchment as a function of mean seasonal discharge.

Table 6

Weathering rates of minerals ( $\text{pmol m}^{-2} \text{ s}^{-1}$ ) in nanocatchment soil expressed relative to mineral surface area (after Clow, 1992; Drever and Clow, 1996)

	Discharge ( $\text{mm d}^{-1}$ )	Oligoclase	Biotite	K-spar
Nanocatchment				
1990	0.90	0.091	0.002	0.006
1991	3.95	0.324	0.012	0.020
1992	3.56	0.138	0.009	0.003
1993	4.49	0.161	0.011	0.046
1994	2.54	0.120	0.010	0.012

*Laboratory column experiments:*

Lab $T$ ( $^{\circ}\text{C}$ )	0.22	0.06
Corr. to $9^{\circ}\text{C}$ <sup>a</sup>	0.09	0.03

*Laboratory flow-through (fluidized bed) reactor experiments:*

Lab $T$ ( $^{\circ}\text{C}$ )	1.84	0.09
Corr. to $9^{\circ}\text{C}$ <sup>a</sup>	0.77	0.04

<sup>a</sup> The temperature correction is based on an activation energy of  $60 \text{ kJ mol}^{-1}$ , the value for the dissolution of albite far from equilibrium (Blum and Stillings, 1996). If the rate-controlling process is transport in solution rather than surface reaction, a much smaller activation energy (and hence temperature correction) would be appropriate.

during each field season at the nanocatchment, which occurs to a greater extent during years of high flow (Clow, 1992). The decline in solute concentrations is likely to occur first in the better-connected micropores because they are more easily flushed. Thus, the concentration gradient between well-connected micropores and the regions of very slowly moving water will increase. Transport of solutes from the slow-flow regions via diffusion should increase in response, providing an additional source of weathering products.

A variety of chemical processes were considered in order to help explain the increased flux of weathering products from the nanocatchment in response to increased water inputs. These include cation exchange, dissolution of amorphous aluminosilicates, desorption of Si from oxide mineral surfaces, and increased mineral weathering rates in response to lower soil solution concentrations.

Cation exchange at the nanocatchment could be driven by inputs of  $\text{H}^{+}$  ion from the atmosphere because it is the largest source of acidity to the

catchment. However, there is no clear correlation between fluxes of  $H^+$  ion in precipitation and total water flux ( $r^2 = 0.16$ ). Microbial processes in the soil, influenced by changes in the hydrologic regime, could also be significant sources of  $H^+$  to displace  $Ca^{2+}$ .

Dissolution of amorphous aluminosilicate material might be an important source of dissolved Si in outflow water at the nanocatchment. Soil solutions at the nanocatchment during August–September 1990 were oversaturated with respect to kaolinite, gibbsite, and amorphous aluminum hydroxide, but were slightly undersaturated with respect to amorphous aluminosilicate (Clow, 1992), indicating that dissolution of amorphous aluminosilicate was favored at that time. The existence of amorphous aluminosilicates in Loch Vale soils is supported by the work of Mast (1989, 1992), who extracted amorphous material from Loch Vale soils and determined that it had the approximate composition  $Al_2Si_2O_5(OH)_4$  (kaolinite). It seems likely that some Si released from weathering of primary silicate minerals during fall and winter, when flow rates were low, formed metastable amorphous aluminosilicates. Some of these amorphous aluminosilicate might eventually form crystalline secondary minerals such as kaolinite, but a substantial portion of it probably redissolved in the summer when soils were flushed with dilute precipitation and deionized irrigation water. Adsorption and desorption of  $SiO_2$  on mineral surfaces is likely to follow the same seasonal pattern, with Si released from primary minerals adsorbing to surfaces in fall and winter when soil solutions were relatively concentrated, and desorbing in the summer when soils were flushed. These seasonal processes are likely to be manifested as an excess of Si in the mass balance in this study, because only the summer period was considered.

Under low-flow conditions, the residence time of solutions in micropores in some cases might be sufficient for solute concentrations to build up enough to decrease dissolution rates via the chemical affinity effect (Burch et al., 1993), that is to say the approach to chemical equilibrium. Burch et al. (1993) in experiments at 80°C and pH 8 showed that reaction rates decreased at surprisingly high degrees of undersaturation. Unfortunately, there are no data on the chemical affinity effect under conditions (tempera-

ture and solution composition) representative of the natural soil environment (Drever and Clow, 1996).

At the nanocatchment, the saturation index ( $\log IAP/K_{sp}$ ) in outflow solutions for phlogopite (a mica with similar composition to biotite), albite (a surrogate for oligoclase), and calcite were  $-43$ ,  $-4.3$ , and  $-3.4$ , respectively, and solutions were near saturation with respect to microcline (Drever and Clow, 1996). If the chemical affinity effect were the dominant control on dissolution rates at the nanocatchment and minerals responded in a similar manner, as flow rates increase one would expect a dramatic increase in microcline dissolution rates, a lesser increase for calcite and oligoclase, and no increase for biotite. This pattern was not observed; as noted previously, calcite and biotite exhibited the largest responses to changes in mean seasonal discharge (Fig. 4). These results indicate that approach to saturation is not the main limiting factor on the flux of weathering products from the soil, except perhaps for microcline.

#### 4. Conclusions

Weathering rates, as calculated from fluxes of weathering products from the soil, are dependent on the rate of water infiltration and flow through the soil. Increased fluxes of weathering products under high flow conditions are best explained by increased transport of solutes from micropores in the soil. Dissolution of amorphous aluminosilicates or desorption of Si from mineral surfaces may provide an important additional source of Si. High water input rates will tend to increase pore water velocities and enhance soil water flushing. In the heterogeneous environment of the soil matrix, pore spaces vary in size and connectivity. The fraction of pores that are flushed during an annual hydrologic season might be a continuous variable that is positively related to the duration and rate of water inputs. The increased flushing will tend to lower solute concentrations in the soil matrix, which will stimulate diffusion from stagnant zones in the soil such as “dead-end” pore spaces and microcracks on mineral surfaces. Lower solute concentrations in the soil matrix might also enhance chemical weathering rates of some silicate minerals, especially microcline. Thus, both physical

transport of solutes and subsequent chemical effects are likely to be responsible for the positive relation observed between fluxes of weathering products and water input rates.

## Acknowledgements

This research was funded by the U.S. Geological Survey through its study of Water, Energy, and Biogeochemical Budgets.

## References

- Arthur, M., 1992. Vegetation. In: J. Baron (Editor), *Biogeochemistry of an Alpine Ecosystem*. Springer, New York, N.Y., pp. 76–92.
- Baron, J., Walthall, P.M., Mast, M.A. and Arthur, M.A., 1992. Soils. In: J. Baron (Editor), *Biogeochemistry of an Alpine Ecosystem*. Springer, New York, N.Y., pp. 108–141.
- Beven, K. and Germann, P., 1982. Macropores and water flow in soils. *Water Resour. Res.*, 18: 1311–1325.
- Birkeland, P.W., Burke, R.M. and Shroba, R.R., 1987. Holocene soils in gneissic cirque deposits, Colorado Front Range. *U.S. Geol. Surv., Bull.*, 1590: E1–E21.
- Blum, A. and Stillings, L.L., 1996. Dissolution kinetics of feldspars. In: S. Brantley and A. White (Editors), *Chemical Weathering Rates of Silicate Minerals*. Mineral. Soc. Am., *Rev. Mineral.*, 31 (in press).
- Braddock, W.A. and Cole, J.C., 1990. *Geologic Map of Rocky Mountain National Park and Vicinity, Colorado*. U.S. Geol. Surv. Map I-1973.
- Brady, P.V. and Walther, J.V., 1990. Kinetics of quartz dissolution at low temperatures. *Chem. Geol.*, 82: 253–264.
- Brunauer, S., Emmett, P.H. and Teller, E., 1938. Adsorption of gases in multimolecular layers. *J. Am. Chem. Soc.*, 60: 309–319.
- Brusseau, M.L., 1993. The influence of solute size, pore water velocity and intraparticle porosity on solute dispersion and transport in soil. *Water Resour. Res.*, 29: 1071–1080.
- Burch, T.E., Nagy, K.L. and Lasaga, A.C., 1993. Free energy dependence of albite dissolution kinetics at 80°C and pH 8.8. *Chem. Geol.*, 105: 137–162.
- Clow, D.W., 1992. Weathering rates from field and laboratory experiments on naturally weathered soils. Ph.D. Dissertation, University of Wyoming, Laramie, Wyo. (unpublished).
- Clow, D.W. and Mast, M.A., 1995. Composition of precipitation, bulk deposition, and runoff at a granitic bedrock catchment in the Loch Vale Watershed, Colorado, USA. In: K.A. Tonnessen, M.W. Williams and M. Tranter (Editors), *Biogeochemistry of Seasonally Snow-covered Catchments*. Int. Assoc. Hydrogeol. Sci. Publ., 228: 235–242.
- Cole, J.C., 1977. *Geology of East-Central Rocky Mountain National Park and vicinity, with emphasis on the emplacement of the Precambrian Silver Plume Granite in the Longs Peak–St. Vrain batholith*. Ph.D. Dissertation, University of Colorado, Boulder, Colo. (unpublished).
- Drever, J.I. and Clow, D.W., 1996. Weathering rates in catchments. In: S. Brantley and A. White (Editors), *Chemical Weathering Rates of Silicate Minerals*. Mineral. Soc. Am., *Rev. Mineral.*, 31 (in press).
- Garrels, R.M. and Mackenzie, F.T., 1967. Origin of the compositions of some springs and lakes. In: W. Stumm (Editor), *Equilibrium Concepts in Natural Water Systems*. Am. Chem. Soc., *Adv. Chem. Ser.*, 67: 222–242.
- Gatz, D.F., Barnard, W.R. and Stensl, G.J., 1986. The role of alkaline materials in precipitation chemistry: a brief review of the issues. *Water Air Soil Pollut.*, 30: 245–251.
- Hornberger, G.M., Beven, K.J. and Germann, P.F., 1990. Inferences about solute transport in macroporous forest soils from time series models. *Geoderma*, 46: 249–262.
- Jackson, M.L., 1969. *Soil Chemical Analysis—Advanced Course*. Dep. Soil Sci., Univ. of Wisconsin, Madison, Wis.
- Linsley, Jr., R.K., Kohler, M.A. and Paulhus, J.L.H., 1982. *Hydrology for Engineers*. McGraw-Hill, New York, N.Y., 3rd ed., 508 pp.
- Lovering, T.S. and Engel, C., 1967. Translocation of silica and other elements from rock into Equisetum and three grasses. *U.S. Geol. Surv., Prof. Pap.*, 594-B, 16 pp.
- Madole, R.F., 1976. Glacial geology of the Front Range, Colorado. In: W.C. Mahaney (Editor), *Quaternary Stratigraphy of North America*. Dowden, Hutchinson and Ross, Stroudsburg, Pa., pp. 297–318.
- Mast, M.A., 1989. A laboratory and field study of chemical weathering with special reference to acid deposition. Ph.D. Dissertation, University of Wyoming, Laramie, Wyo. (unpublished).
- Mast, M.A., 1992. Geochemical characteristics. In: J. Baron (Editor), *Biogeochemistry of an Alpine Ecosystem*. Springer, New York, N.Y., pp. 93–107.
- Mast, M.A., Drever, J.I. and Baron, J., 1990. Chemical weathering in the Loch Vale watershed, Rocky Mountain National Park, Colorado. *Water Resour. Res.*, 26: 2971–2978.
- Network, N.A.D.P.N.T., 1984–1994. Annual data summary, precipitation chemistry in the United States. NADP/NTN (Natl. Atmos. Deposition Prog./Natl. Trends Network) Coord. Off., Nat. Resour. Ecol. Lab., Colorado State Univ., Fort Collins, Colo.
- Penman, H.L., 1948. Natural evapotranspiration from open water, bare soil, and grass. *Proc. R. Soc. London, Ser. A*, 193: 120–145.
- Swoboda-Colberg, N.G. and Drever, J.I., 1993. Mineral dissolution rates in plot-scale field and laboratory experiments. *Chem. Geol.*, 105: 51–69.
- Velbel, M.A., 1993. Constancy of silicate-mineral weathering-rate ratios between natural and experimental weathering: implications for hydrologic control of differences in absolute rates. *Chem. Geol.*, 105: 89–99.
- White, A.F. and Blum, A., 1995. Effects of climate on chemical weathering in watersheds. *Geochim. Cosmochim. Acta.*, 59: 1729–1747.